Control of Stress-Dependent Cardiac Growth and Gene Expression by a MicroRNA

Eva van Rooij *et al.*

Science **316**, 575 (2007);
DOI: 10.1126/science.1139089

Control of Stress-Dependent Cardiac Growth and Gene Expression by a MicroRNA

Eva van Rooij,[1] Lillian B. Sutherland,[1] Xiaoxia Qi,[1] James A. Richardson,[1,2] Joseph Hill,[3] Eric N. Olson[1]*

The heart responds to diverse forms of stress by hypertrophic growth accompanied by fibrosis and eventual diminution of contractility, which results from down-regulation of α–myosin heavy chain (αMHC) and up-regulation of βMHC, the primary contractile proteins of the heart. We found that a cardiac-specific microRNA (miR-208) encoded by an intron of the *αMHC* gene is required for cardiomyocyte hypertrophy, fibrosis, and expression of *βMHC* in response to stress and hypothyroidism. Thus, the *αMHC* gene, in addition to encoding a major cardiac contractile protein, regulates cardiac growth and gene expression in response to stress and hormonal signaling through miR-208.

Cardiac contractility depends on the expression of two *MHC* genes, α and β, which are regulated in an antithetical manner by developmental, physiological, and pathological signals. βMHC, a relatively slow adenosine triphosphatase (ATPase), is the dominant isoform expressed in the embryonic heart, whereas αMHC, a fast ATPase, is up-regulated postnatally (*1*). Thyroid hormone (T3) signaling stimulates *αMHC* and inhibits *βMHC* transcription after birth (*2*). In contrast, hypothyroidism and various forms of cardiac stress increase βMHC expression with consequent diminution in cardiac performance (*3*–*5*). αMHC is the major adult cardiac isoform in rodents, whereas βMHC is the predominant isoform in adult human hearts and becomes even more abundant during cardiac disease when αMHC is down-regulated (*6*–*9*). Because even relatively subtle variations in the ratio of αMHC and βMHC can profoundly influence cardiac function, there has been great interest in deciphering the mechanisms that coordinate αMHC and βMHC expression and in strategies to therapeutically manipulate cardiac MHC expression (*10*).

MicroRNAs (miRNAs) are small, non–protein-coding RNAs that base pair with specific mRNAs and inhibit translation or promote mRNA degradation (*11*). MiRNAs arise from primary transcripts of variable sizes that are processed into 70- to 100-nucleotide hairpin-shaped precursors, which are processed into mature miRNAs of

[1]Department of Molecular Biology, University of Texas Southwestern Medical Center, Dallas, TX 75390–9148, USA. [2]Department of Pathology, University of Texas Southwestern Medical Center, Dallas, TX 75390–9148, USA. [3]Department of Internal Medicine, University of Texas Southwestern Medical Center, 6000 Harry Hines Boulevard, Dallas, TX 75390–9148, USA.

*To whom correspondence should be addressed. E-mail: eric.olson@utsouthwestern.edu

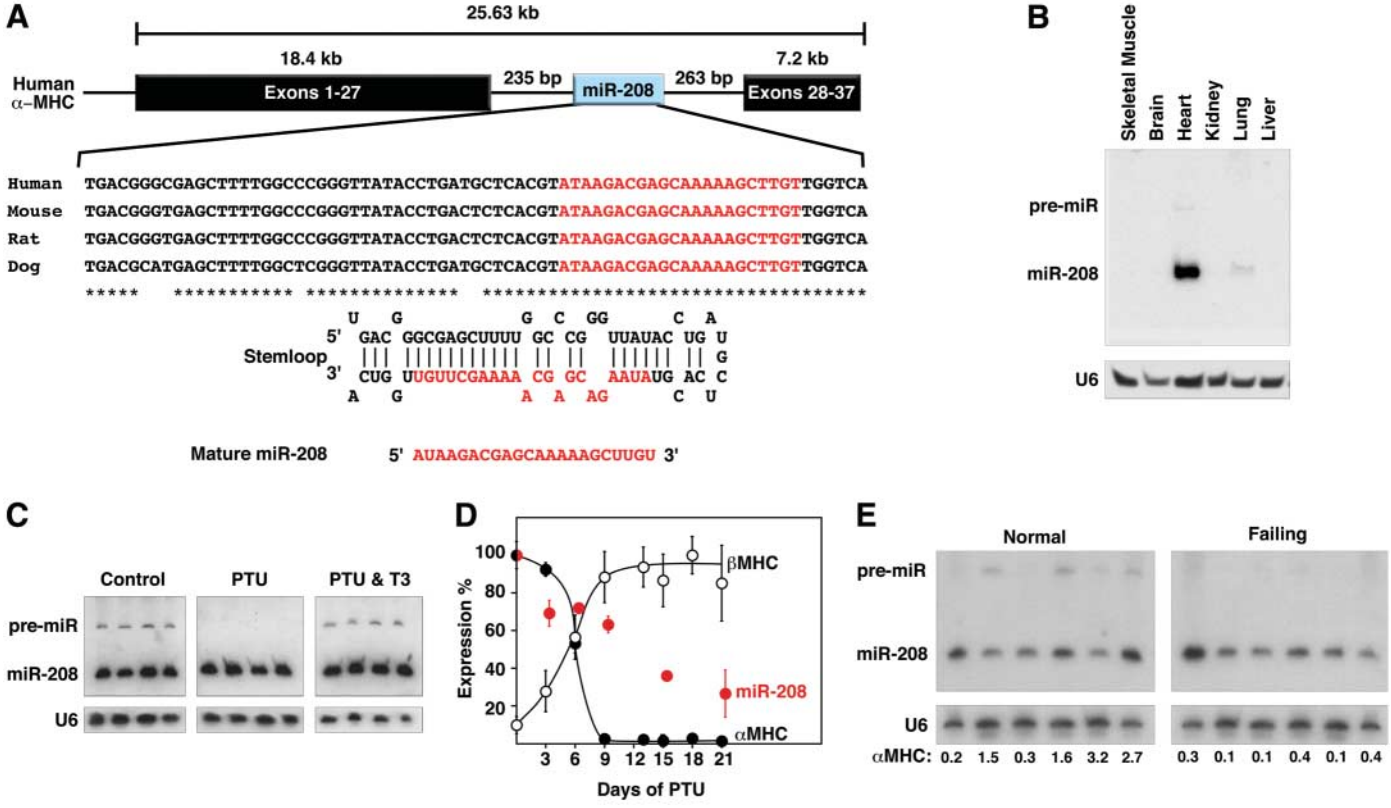

Fig. 1. Expression of miR-208 and coregulation with αMHC. (**A**) MiR-208 is encoded by intron 27 of the *αMHC* gene. Asterisks indicate sequence conservation. (**B**) Detection of miR-208 transcripts by Northern analysis of adult mouse tissues. U6 mRNA serves as a loading control. (**C**) Rats were treated with PTU or PTU + T3, as indicated, for a week, and the expression of miR-208 was detected by Northern blot. Hearts from four animals under each condition were analyzed. (**D**) Transcripts for *αMHC* and *βMHC* and miR-208 were quantified by real-time polymerase chain reaction (PCR) analysis at the indicated times after treatment with PTU. Expression of the miR-208 pre-miRNA parallels that of *αMHC* gene expression, whereas the mature miR-208 continues to be expressed even after the disappearance of *αMHC* mRNA. Values represent mean ± SEM of hearts of four animals at each time point. (**E**) Transcripts for *αMHC* and miR-208 were detected by Northern blot of cardiac tissue from six normal individuals and six individuals with idiopathic cardiomyopathy. Indicated αMHC levels were relative to average expression level in normal hearts. There is a close correlation between the level of expression of *αMHC* and pre–miR-208, whereas mature miR-208 expression is maintained after the latter RNAs have been down-regulated.

18 to 25 nucleotides. MiRNAs that base pair perfectly with target mRNA sequences result in mRNA degradation, whereas those that display imperfect sequence complementarity with target mRNAs generally result in translational inhibition (*12*). Overexpression experiments have implicated miRNAs in diverse cellular processes (*13*–*19*), but to date, there have been no reports of the consequences of deletion of miRNA genes in vertebrate organisms. Recently, we identified a signature pattern of miRNAs associated with pathological cardiac growth and remodeling (*19*). Here, we describe miR-208 as an essential cardiac-specific regulator of β*MHC* expression and mediator of stress and T3 signaling in the heart.

Regulation of miR-208 expression. MiR-208 is encoded by intron 27 of the human and mouse α*MHC* gene. The sequences of miR-208 found in humans, mice, rats, and dogs are identical and the pre-miRNA is highly conserved in mammals (Fig. 1A). Consistent with the specific expression of αMHC in the heart and the pulmonary myocardium (*20*), miR-208 is expressed specifically in the heart and at trace levels in the lung (Fig. 1B). Blockade of T3 biosynthesis with propylthiouracil (PTU) represses α*MHC* and induces β*MHC* expression (*21*). After rats were treated with PTU for one week, the expression of α*MHC* mRNA declined in parallel with the level of the miR-208 stem loop, whereas mature miR-208 showed little or no change in expression. T3 treatment blocked the effects of PTU on expression of α*MHC* mRNA and pre–miR-208 (Fig. 1C and fig. S1A).

A time course of PTU treatment showed that α*MHC* and pre–miR-208 expression decreased and β*MHC* increased during the first 9 days of PTU treatment (Fig. 1D and fig. S1, B and C). Expression of pre–miRNA-208 paralleled α*MHC* mRNA expression, whereas even after 21 days of PTU treatment, long after α*MHC* mRNA expression had ceased, 30% of the mature miR-208 remained (Fig. 1D and fig. S1, B and C). We infer from the coregulation of pre–miR-208 and the α*MHC* transcript that miR-208 is processed from the α*MHC* intron rather than being transcribed as a separate RNA. The sustained expression of miR-208 after the pre-miRNA and α*MHC* transcripts are down-regulated by PTU suggests that it is extremely stable, with a half-life of >12 days.

Although α*MHC* mRNA constitutes only about 30% of total *MHC* mRNA expressed in normal adult human heart (*8*), miR-208 expression was readily detectable in human cardiac tissue (Fig. 1E). Consistent with its relatively long half-life, miR-208 was also detectable in idiopathic failing human hearts in which αMHC levels were diminished relative to normal hearts.

Generation of miR-208 mutant mice. We deleted the miR-208 coding region by introducing loxP sites for Cre-mediated recombination at both ends of an 83–base pair (bp) region of intron 27 of the mouse α*MHC* gene, which encodes the complete pre-miRNA sequence of miR-208 (Fig. 2A and fig. S2A). Breeding of miR-208$^{loxP/+}$ mice to mice bearing a ubiquitously expressed Cre recombinase transgene resulted in deletion of the miR-208 genomic sequence and the complete absence of miR-208 in homozygous mutant animals (Fig. 2B and fig. S2B). Disruption of the α*MHC* gene causes early embryonic lethality (*22*). Thus, it was important that the miR-208 targeting strategy not alter α*MHC* transcription or splicing. Deletion of miR-208 did not interfere with α*MHC* mRNA splicing or alter the expression of αMHC or βMHC proteins in hearts of newborn mice (Fig. 2C and fig. S2, C and D). A Western blot using an antibody against all striated myosins indicated no visible differences between wild-type and miR-208 mutant animals (fig. S3A).

Mice homozygous for the miR-208 deletion were viable and did not display obvious abnormalities in size, shape, or structure of the heart up to 20 weeks of age. Analysis of cardiac function by echocardiography showed a slight reduction in contractility, measured by fractional shortening, in miR-208$^{-/-}$ animals compared with the contractility of wild-type littermates at 2 months of age, which was attributable primarily to an increase in left ventricular diameter during systole (fig. S3B). At advanced age (>6 months), cardiac function declined further in mutant animals as a result of abnormalities in sarcomere structure.

Microarray analysis on hearts from wild-type and miR-208$^{-/-}$ animals at 2 months of age revealed that the removal of miR-208 resulted in pronounced expression of fast skeletal muscle contractile protein genes, including those encoding Troponin I2, Troponin T3, and myosin light chain-alkali, which are normally not expressed in the heart. Transcripts encoding the natriuretic peptides atrial natriuretic factor (ANF) and b-type natriuretic peptide (BNP), and heat shock proteins, which serve as markers of cardiac stress, were also up-regulated in the hearts of miR-208$^{-/-}$ animals (fig. S3, C and D, and table S1). None of the up-regulated transcripts contained predicted target sequences for miR-208, suggesting that they are regulated indirectly by miR-208.

MiR-208 regulates βMHC expression and cardiac remodeling. To further investigate the potential functions of miR-208, we compared the response of wild-type and miR-208 mutant mice to thoracic aortic banding (TAB), which induces cardiac hypertrophy by increased afterload on the heart and is accompanied by down-regulation of α*MHC* and up-regulation of β*MHC* (*23*). α*MHC* mRNA expression declined as expected after TAB (fig. S4A), but miR-208 was still abundantly expressed 21 days after TAB (fig. S4B), consistent with its relatively long half-life.

In response to TAB, wild-type mice showed a pronounced increase in cardiac mass accompanied by hypertrophic growth of cardiomyocytes

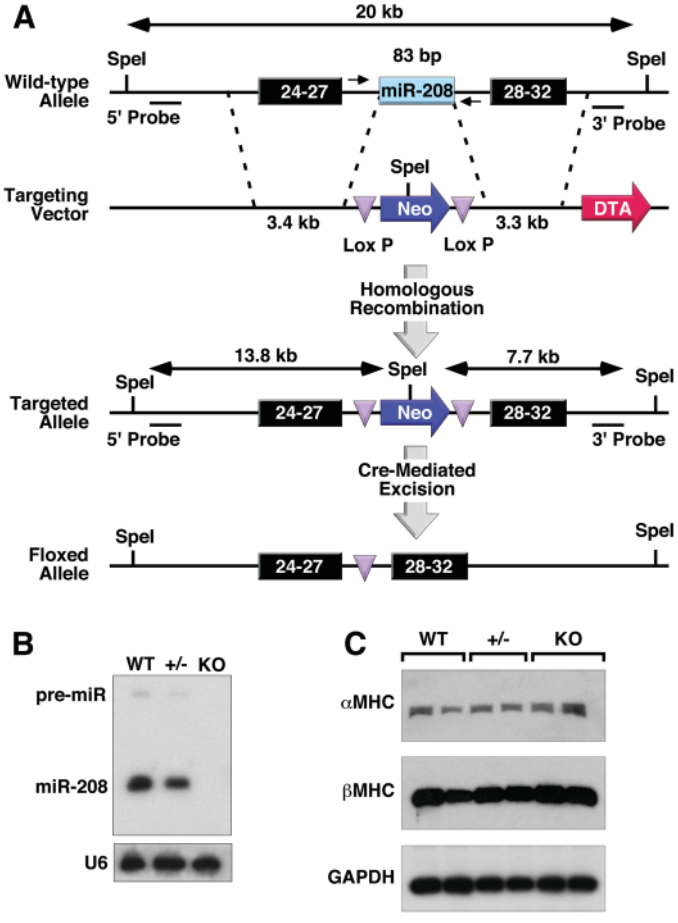

Fig. 2. Generation of miR-208 mutant mice. (**A**) Strategy to generate miR-208 mutant mice by homologous recombination. The pre-miRNA sequence was replaced with a neomycin resistance cassette (Neo) flanked by loxP sites. The neomycin cassette was removed in the mouse germ line by breeding heterozygous mice to transgenic mice harboring the CAG-Cre transgene. DTA, diphtheria toxin A. (**B**) Detection of miR-208 transcripts by Northern analysis of hearts from wild-type (WT) and miR-208 mutant (KO) mice. (**C**) Western analysis of αMHC and βMHC protein levels in hearts of neonatal mice of the indicated genotypes. Two mice of each genotype were analyzed. Glyceraldehyde-3-phosphate dehydrogenase (GAPDH) was detected as a loading control.

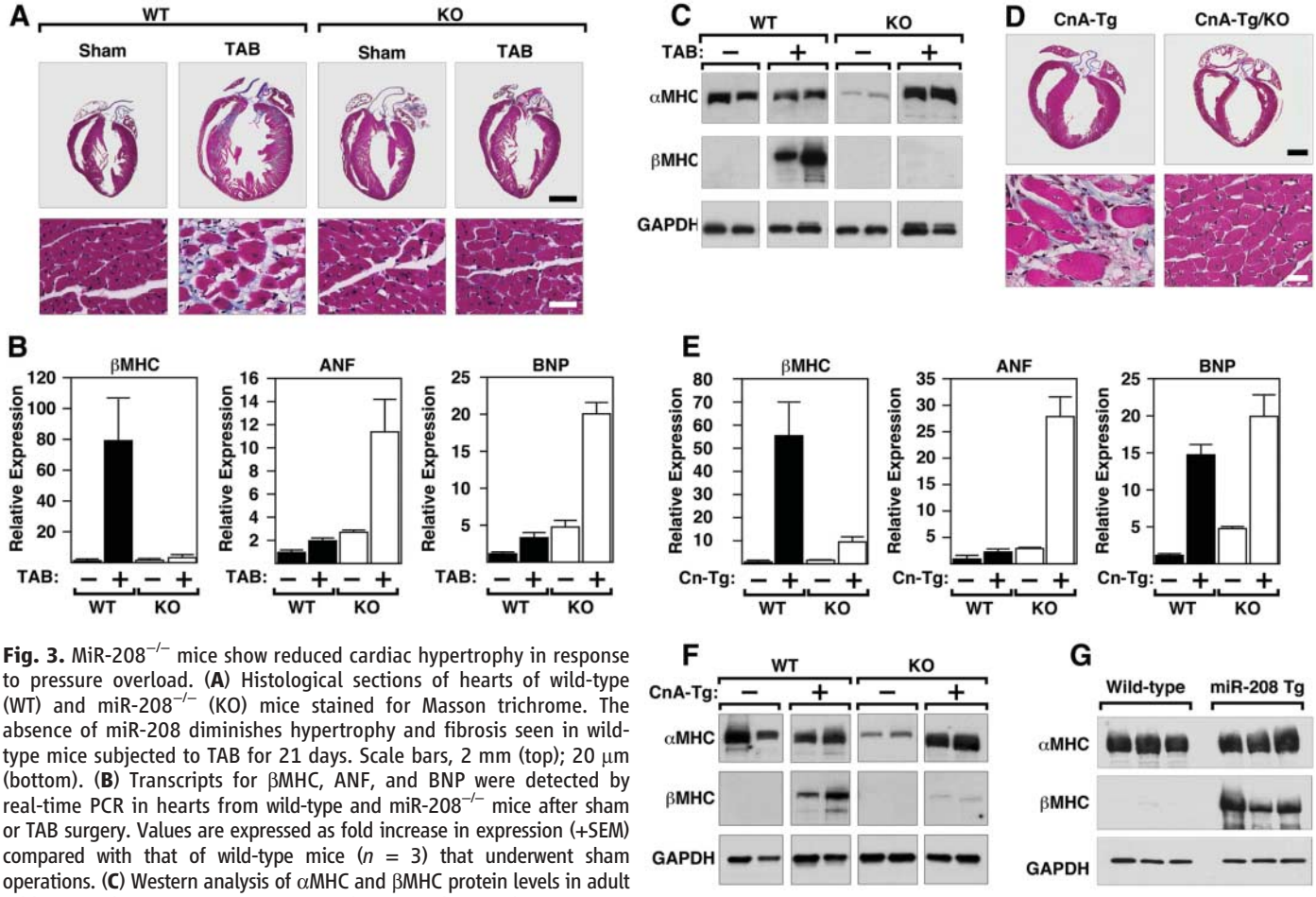

Fig. 3. MiR-208$^{-/-}$ mice show reduced cardiac hypertrophy in response to pressure overload. (**A**) Histological sections of hearts of wild-type (WT) and miR-208$^{-/-}$ (KO) mice stained for Masson trichrome. The absence of miR-208 diminishes hypertrophy and fibrosis seen in wild-type mice subjected to TAB for 21 days. Scale bars, 2 mm (top); 20 μm (bottom). (**B**) Transcripts for βMHC, ANF, and BNP were detected by real-time PCR in hearts from wild-type and miR-208$^{-/-}$ mice after sham or TAB surgery. Values are expressed as fold increase in expression (+SEM) compared with that of wild-type mice (n = 3) that underwent sham operations. (**C**) Western analysis of αMHC and βMHC protein levels in adult wild-type and miR-208 mutant mice 21 days after sham and TAB surgery. (**D**) Histological sections of hearts of 6-week-old mice expressing a calcineurin transgene (CnA-Tg) and hearts of miR-208$^{-/-}$; CnA-Tg mice stained for Masson trichrome. The absence of miR-208 diminishes hypertrophy and fibrosis seen in CnA-Tg mice. Scale bars, 2 mm (top); 20 μm (bottom). (**E**) Transcripts for βMHC, ANF, and BNP were detected by real-time PCR in hearts from the indicated genotype. Values are expressed as fold increase in expression (+SEM) compared with that of wild-type mice (n = 3). (**F**) Western analysis of αMHC and βMHC protein levels in adult wild-type and miR-208 mutant mice with and without the presence of the CnA transgene. (**G**) Western analysis of αMHC and βMHC protein levels in adult wild-type and miR-208 transgenic animals.

and ventricular fibrosis (Fig. 3A). In contrast, miR-208 mutant animals showed virtually no hypertrophy of cardiomyocytes or fibrosis in response to TAB (Fig. 3A). Echocardiography confirmed that miR-208$^{-/-}$ animals displayed a blunted hypertrophic response and a reduction in contractility (fig. S4C). Most notably, mutant animals were unable to up-regulate βMHC. Instead, αMHC protein expression increased in miR-208 mutant hearts in response to TAB, which may reflect a compensatory mechanism to maintain MHC expression in the absence of βMHC up-regulation. Other stress-responsive genes, such as those encoding the natriuretic peptides ANF and BNP, were strongly induced in miR-208 mutant animals (Fig. 3, B and C). Microarray analysis on hearts from wild-type and miR-208$^{-/-}$ animals confirmed that the absence of miR-208 resulted in a highly specific block to βMHC expression (table S2).

MiR-208$^{-/-}$ mice were also resistant to fibrosis and cardiomyocyte hypertrophy in response to transgenic expression of activated calcineurin (Fig. 3D), an especially powerful stimulus for cardiac hypertrophy and heart failure (*24*). Similarly, β*MHC* mRNA and protein failed to be up-regulated in hearts of miR-208$^{-/-}$;calcineurin transgene mice at 6 weeks of age, whereas ANF and BNP were strongly induced (Fig. 3, E and F). Thus, miR-208 is necessary for up-regulation of β*MHC* and cellular remodeling, but not for expression of other markers of cardiac stress.

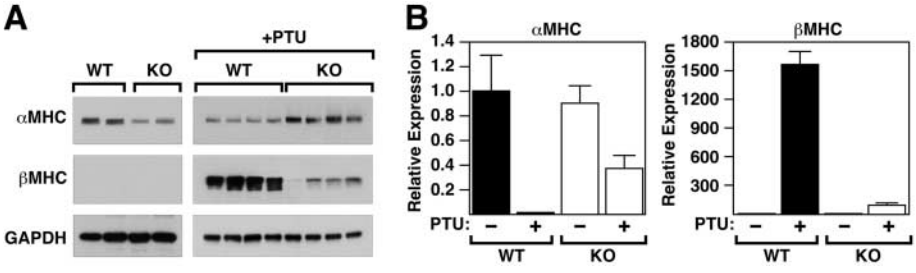

Fig. 4. Regulation of thyroid hormone responsiveness of the β*MHC* gene by miR-208. (**A**) Western analysis of αMHC and βMHC expression in wild-type (WT) and miR-208 mutant (KO) mice at baseline and 2 weeks after PTU treatment. (**B**) Transcripts for α*MHC* and β*MHC* were detected by real-time PCR in hearts from wild-type and miR-208$^{-/-}$ mice after PTU treatment. Values are expressed as fold increase in expression (+SEM) compared with that of wild-type mice that received regular chow (n = 3).

To test whether miR-208 was sufficient for up-regulation of β*MHC* expression, we generated transgenic mice that overexpressed miR-208 under control of the α*MHC* promoter. α*MHC–miR-208* transgenic mice were viable, and their miR-208 expression was about three times as high as that of wild-type hearts (fig. S4D). Hearts from a transgenic line representing the average over-

expression of the transgene showed no overt signs of pathological remodeling at 2 months of age but, notably, displayed a marked up-regulation of β*MHC* expression (Fig. 3G and fig. S4E). This activity of miR-208 was specific, as shown by transgenic overexpression of miR-214, which is induced during cardiac hypertrophy (*19*), but had no effect on β*MHC* expression. Because the endogenous level of miR-208 in the adult mouse heart is insufficient to up-regulate β*MHC* expression, the finding that a threefold increase in miR-208 expression in these transgenic mice results in up-regulation of β*MHC* expression suggests that there is a sharp threshold for the control of β*MHC* expression by this microRNA.

MiR-208 regulates T3-dependent repression of β*MHC*. T3 signaling induces α*MHC* transcription through a positive T3 response element (TRE), whereas a negative TRE in the promoter of the β*MHC* gene mediates transcriptional repression (*25*). To test whether miR-208 was required for T3-dependent regulation of β*MHC*, we fed mutant and wild-type littermates PTU-containing chow for 2 weeks to block T3 signaling. Northern blot analysis verified that miR-208 was abundantly present after 2 weeks of PTU treatment (fig. S5A). PTU, as expected, induced a decline in heart rate and contractility and an increase in dilation, with no marked differences between wild-type and mutant animals (fig. S5B). However, whereas wild-type animals showed the expected decrease in α*MHC* and increase in β*MHC* in response to PTU, the miR-208$^{-/-}$ animals again appeared resistant to up-regulation of β*MHC*, although a trace of β*MHC* expression was detectable (Fig. 4). *ANF* and *BNP* were up-regulated by PTU in miR-208$^{-/-}$ animals, confirming the specific role of miR-208 in β*MHC* expression (fig. S5C). Because PTU induces the α*MHC*-to-β*MHC* isoform switch by interfering solely with thyroid hormone receptor (TR) signaling (*21*), these findings suggest that miR-208 potentiates β*MHC* expression through a mechanism involving the TR.

MiR-208 targets TR-Associated Protein 1. Among the relatively few predicted targets of miR-208, the mRNA encoding thyroid hormone receptor Associated Protein 1 (THRAP1), also known as TRAP240, scored as the strongest predicted target with the PicTar target-prediction program (*26*). THRAP1, a component of the TR-associated TRAP complex, modulates activity of the TR by recruitment of RNA polymerase II and general initiation factors (*27*). The putative miR-208 binding site in the 3′ untranslated region (UTR) of the *THRAP1* mRNA showed high complementarity with the 5′ arm of miR-208, the most critical determinant of miRNA targeting, as well as evolutionary conservation (Fig. 5A). Based on the imperfect complementarity of miR-208 and *THRAP1* 3′-UTR sequence, miR-208 would be expected to inhibit translation of *THRAP1*.

To test whether the putative miR-208 target sequence in the *THRAP1* 3′ UTR could mediate translational repression, we inserted the full length 3′ UTR of the *THRAP1* transcript into a luciferase expression plasmid, which we transfected into COS1 cells. Increasing amounts of CMV-driven miR-208 resulted in a dose-dependent decrease in luciferase activity, whereas comparable amounts of miR-126, which served as a control, had no effect (Fig. 5B). CMV–miR-208 also dose-dependently abrogated translation of a hemagglutinin (HA)–tagged malonyl coenzyme A decarboxylase (MCD) expression cassette linked to the *THRAP1* 3′-UTR binding sequence, but not a mutant miR-208 target sequence (Fig. 5C). In addition, THRAP1 protein expression was increased in cardiac protein lysates from miR-208$^{-/-}$ mice compared with that in wild-type littermates (Fig. 5D), whereas THRAP1 mRNA was comparable in hearts of the two genotypes (fig. S6), consistent with the conclusion that miR-208 acts as a negative regulator of THRAP1 translation in vivo. Under situations of stress, the negative influence of miR-208 on THRAP1 protein expression may be even greater, in light of recent studies showing that stress augments repressive actions of miRNAs by promoting the association of miRNAs with Argonaute (*28*).

Discussion. Our results demonstrate that miR-208, which is encoded by an intron of the α*MHC* gene, regulates stress-dependent cardiomyocyte growth and gene expression. In the

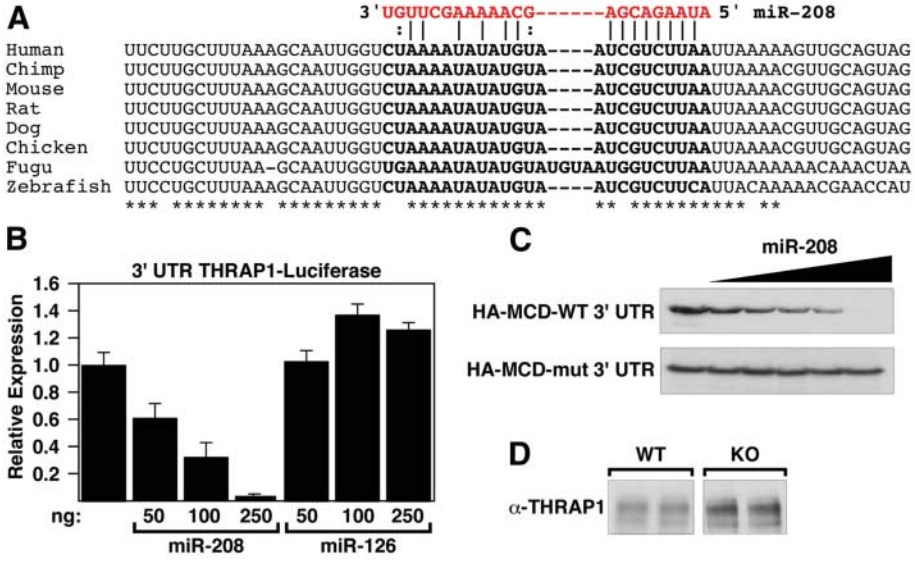

Fig. 5. MiR-208 targets THRAP1. (**A**) Sequence alignment of putative miR-208 binding site in 3′ UTR of *THRAP1* shows a high level of complementarity and sequence conservation. (**B**) COS1 cells were transfected with a *THRAP1* 3′-UTR luciferase construct, along with expression plasmids for miR-126 and miR-208. Values are fold change in luciferase expression (+SD) compared with the reporter alone. (**C**) COS1 cells were transfected with either HA-MCD—wild-type (WT) UTR or HA-MCD-mutated UTR along with increasing dosages of pCMV—miR-208 ranging from 0.1 to 2 μg. HA levels were detected using immunoblot. (**D**) THRAP1 Western blot using a THRAP1 specific antibody on THRAP1-immunoprecipitated cardiac cell lysates using 400 μg of protein from either wild-type or miR-208$^{-/-}$ (KO) animals.

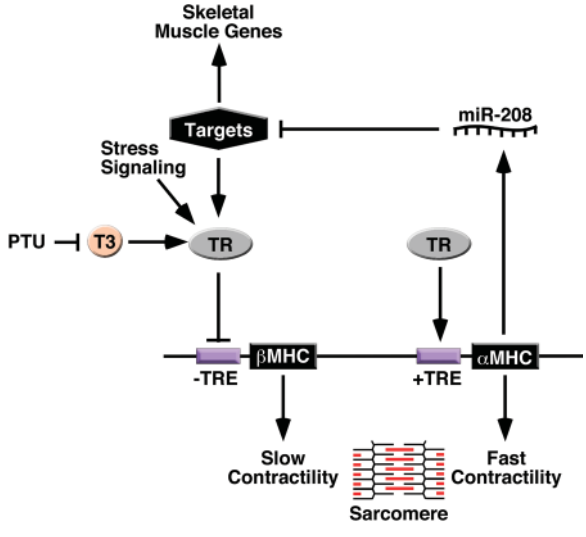

Fig. 6. A model for the role of miR-208 in cardiac gene regulation. The αMHC gene encodes miR-208, which negatively regulates expression of THRAP1 and skeletal muscle genes (and probably additional targets). The α*MHC* and β*MHC* genes are linked and miR-208 is required for up-regulation of β*MHC* in response to stress signaling and blockade to T3 signaling by PTU. αMHC and βMHC promote fast and slow contractility, respectively.

absence of miR-208, the expression of β*MHC* is severely blunted in the adult heart in response to pressure overload, activated calcineurin, or hypothyroidism, suggesting that the pathways through which these stimuli induce β*MHC* transcription share a common miR-208–sensitive component (Fig. 6). In contrast, β*MHC* expression was unaltered in the hearts of newborn miR-208$^{-/-}$ mice, demonstrating that miR-208 participates specifically in the mechanism for stress-dependent regulation of β*MHC* expression.

A clue to the mechanism of action of miR-208 comes from the resemblance of miR-208$^{-/-}$ hearts to hyperthyroid hearts, both of which display a block to βMHC expression, up-regulation of stress-response genes (*29*, *30*), and protection against pathological hypertrophy and fibrosis (*31*, *32*). The up-regulation of fast skeletal muscle genes in miR-208$^{-/-}$ hearts also mimics the induction of fast skeletal muscle fibers in the hyperthyroid state (*33*). T3 signaling represses β*MHC* expression in the postnatal heart, and PTU, which causes hypothyroidism, induces β*MHC* (*2*, *21*). The inability of PTU to induce β*MHC* expression in miR-208$^{-/-}$ hearts further implicates miR-208 in the T3 signaling pathway.

Our results suggest that miR-208 acts, at least in part, by repressing expression of the TR coregulator THRAP1, which can exert positive and negative effects on transcription (*34*, *35*). The TR acts through a negative TRE to repress β*MHC* expression in the adult heart (*2*). Thus, the increase in THRAP1 expression in the absence of miR-208 would be predicted to enhance the repressive activity of the TR toward β*MHC* expression, consistent with the blockade to β*MHC* expression in miR-208$^{-/-}$ hearts. In contrast, the regulation of α*MHC* and β*MHC* expression during development is independent of T3 signaling (*2*) and is unaffected by miR-208. Notably, other TR target genes, such as *phospholamban* and *sarco(endo)plasmic reticulum calcium ATPase 2a* and *glucose transporter 4* were expressed normally in miR-208$^{-/-}$ mice (fig. S7). It has been proposed that the β*MHC* gene may respond to specific TR isoforms (*36*–*38*). Perhaps THRAP1 acts on specific TR isoforms or selectively on a subset of TR-dependent genes through interactions with promoter-specific factors. Because miRNAs generally act through multiple downstream targets to exert their effects, additional targets are also likely to contribute to the effects of miR-208 on cardiac growth and gene expression.

Relatively minor increases in βMHC composition, as occur during cardiac hypertrophy and heart failure, can reduce myofibrillar ATPase activity and systolic function (*9*). Thus, therapeutic manipulation of miR-208 expression or interaction with its mRNA targets could potentially enhance cardiac function by suppressing βMHC expression. Based on the profound influence of miR-208 on the cardiac stress response, and the regulation of numerous miRNAs in the diseased heart (*19*), we anticipate that miRNAs will prove to be key regulators of the functions and responses to disease of the adult heart and possibly other organs.

References and Notes

1. A. Weiss, L. A. Leinwand, *Annu. Rev. Cell Dev. Biol.* **12**, 417 (1996).
2. E. Morkin, *Microsc. Res. Tech.* **50**, 522 (2000).
3. M. Krenz, J. Robbins, *J. Am. Coll. Cardiol.* **44**, 2390 (2004).
4. H. Kiriazis, E. G. Kranias, *Annu. Rev. Physiol.* **62**, 321 (2000).
5. D. Fatkin *et al.*, *J. Clin. Invest.* **106**, 1351 (2000).
6. B. D. Lowes *et al.*, *J. Clin. Invest.* **100**, 2315 (1997).
7. S. Miyata, W. Minobe, M. R. Bristow, L. A. Leinwand, *Circ. Res.* **86**, 386 (2000).
8. K. Nakao, W. Minobe, R. Roden, M. R. Bristow, L. A. Leinwand, *J. Clin. Invest.* **100**, 2362 (1997).
9. W. T. Abraham *et al.*, *Mol. Med.* **8**, 750 (2002).
10. T. A. McKinsey, E. N. Olson, *J. Clin. Invest.* **115**, 538 (2005).
11. D. P. Bartel, *Cell* **116**, 281 (2004).
12. W. P. Kloosterman, R. H. Plasterk, *Dev. Cell* **11**, 441 (2006).
13. A. Esquela-Kerscher, F. J. Slack, *Nat. Rev. Cancer* **6**, 259 (2006).
14. S. Costinean *et al.*, *Proc. Natl. Acad. Sci. U.S.A.* **103**, 7024 (2006).
15. S. M. Hammond, *Curr. Opin. Genet. Dev.* **16**, 4 (2006).
16. V. Ambros, *Cell* **113**, 673 (2003).
17. Y. Zhao, E. Samal, D. Srivastava, *Nature* **436**, 214 (2005).
18. J. F. Chen *et al.*, *Nat. Genet.* **38**, 228 (2006).
19. E. van Rooij *et al.*, *Proc. Natl. Acad. Sci. U.S.A.* **103**, 18255 (2006).
20. A. Subramaniam *et al.*, *J. Biol. Chem.* **266**, 24613 (1991).
21. G. T. Schuyler, L. R. Yarbrough, *Basic Res. Cardiol.* **85**, 481 (1990).
22. W. K. Jones *et al.*, *J. Clin. Invest.* **98**, 1906 (1996).
23. J. A. Hill *et al.*, *Circulation* **101**, 2863 (2000).
24. J. D. Molkentin *et al.*, *Cell* **93**, 215 (1998).
25. K. Ojamaa, A. Kenessey, I. Klein, *Endocrinology* **141**, 2139 (2000).
26. A. Krek *et al.*, *Nat. Genet.* **37**, 495 (2005).
27. M. Ito, R. G. Roeder, *Trends Endocrinol. Metab.* **12**, 127 (2001).
28. A. K. Leung, J. M. Calabrese, P. A. Sharp, *Proc. Natl. Acad. Sci. U.S.A.* **103**, 18125 (2006).
29. T. Wei, C. Zeng, Y. Tian, Q. Chen, L. Wang, *J. Endocrinol. Invest.* **28**, 8 (2005).
30. C. Pantos *et al.*, *Horm. Metab. Res.* **38**, 308 (2006).
31. J. Yao, M. Eghbali, *Circ. Res.* **71**, 831 (1992).
32. W. J. Chen, K. H. Lin, Y. S. Lee, *Mol. Cell. Endocrinol.* **162**, 45 (2000).
33. A. Vadaszova, G. Zacharova, K. Machacova, I. Jirmanova, T. Soukup, *Physiol. Res.* **53**, (suppl. 1), S57 (2004).
34. R. Pavri *et al.*, *Mol. Cell* **18**, 83 (2005).
35. S. W. Park *et al.*, *Mol. Cell* **19**, 643 (2005).
36. K. Kinugawa, C. S. Long, M. R. Bristow, *J. Clin. Endocrinol. Metab.* **86**, 5089 (2001).
37. A. Mansen, F. Yu, D. Forrest, L. Larsson, B. Vennstrom, *Mol. Endocrinol.* **15**, 2106 (2001).
38. K. Kinugawa *et al.*, *Circ. Res.* **89**, 591 (2001).

39. This work was supported by grants from the NIH and the Donald W. Reynolds Cardiovascular Clinical Research Center to E.N.O. We thank C. Plato at Gilead Colorado (Westminster, CO) for providing human and rat RNA samples; M. Arnold for advice; and J. Shelton, J. McAnally, and C. Nolen for technical assistance.

Supporting Online Material

www.sciencemag.org/cgi/content/full/1139089/DC1
Materials and Methods
Figs. S1 to S7
Tables S1 and S2
References

20 December 2006; accepted 7 March 2007
Published online 22 March 2007;
10.1126/science.1139089
Include this information when citing this paper.

REPORTS

Environment-Induced Sudden Death of Entanglement

M. P. Almeida, F. de Melo, M. Hor-Meyll, A. Salles, S. P. Walborn, P. H. Souto Ribeiro, L. Davidovich*

We demonstrate the difference between local, single-particle dynamics and global dynamics of entangled quantum systems coupled to independent environments. Using an all-optical experimental setup, we showed that, even when the environment-induced decay of each system is asymptotic, quantum entanglement may suddenly disappear. This "sudden death" constitutes yet another distinct and counterintuitive trait of entanglement.

The real-world success of quantum computation (*1*, *2*) and communication (*3*–*9*) relies on the longevity of entanglement in multiparticle quantum states. The presence of decoherence (*10*) in communication channels and computing devices, which stems from the unavoidable interaction between these systems and the environment, degrades the entanglement when the particles propagate or the computation evolves. Decoherence leads to local dynamics, associated with single-particle dissipation, diffusion, and decay, as well as to global dynamics, which may provoke the disappearance of entanglement at a finite time (*11*–*15*). This phenomenon, known as "entanglement sudden death" (*15*), is strikingly different from single-particle dynamics, which occurs asymptotically, and has thus stimulated much recent theoretical work (*11*–*15*). Here we demonstrate the sudden death of entanglement of a two-qubit system under the influence of independent environ-

Instituto de Física, Universidade Federal do Rio de Janeiro, Caixa Postal 68528, Rio de Janeiro RJ 21941-972, Brazil.

*To whom correspondence should be addressed. E-mail: ldavid@if.ufrj.br